Spirocyclic derivatives of nitronyl nitroxides in the design of heterospin Cu^{II} complexes manifesting spin transitions

*N. A. Artiukhova,[a,b] K. Yu. Maryunina,[a] S. V. Fokin,[a] E. V. Tretyakov,[a] G. V. Romanenko,[a] A. V. Polushkin,[a,b] A. S. Bogomyakov,[a] R. Z. Sagdeev,[a] and V. I. Ovcharenko[a]**

[a]*International Tomography Center, Siberian Branch of the Russian Academy of Sciences, 3a ul. Institutskaya, 630090 Novosibirsk, Russian Federation. Fax: +7 (383) 333 1399. E-mail: Victor.Ovcharenko@tomo.nsc.ru*
[b]*Novosibirsk State University, 2 ul. Pirogova, 630090 Novosibirsk, Russian Federation*

A method was developed for the synthesis of a nitronyl nitroxide containing cyclopentane substituents in positions 4 and 5 of the imidazoline ring, *viz.*, 2-(3-pyridyl)-4,5-bis(spiropentyl)-4,5-dihydro-1*H*-imidazole-3-oxide-1-oxyl (L^{CP}). The reaction of Cu^{II} hexafluoroacetylacetonate with L^{CP} affords different products depending on the reaction conditions: mononuclear $[Cu(hfac)_2(L^{CP})_2]$, binuclear $[Cu(hfac)_2L^{CP}]_2$, tetranuclear $\{[Cu(hfac)_2]_4(L^{CP})_2\}$, or chain polymer $\{[Cu(hfac)_2]_3(L^{CP})_2\}_n$. Temperature changes induce structural transformations accompanied by a change in the spin state in exchange clusters in the solid $[Cu(hfac)_2L^{CP}]_2$ and $\{[Cu(hfac)_2]_4(L^{CP})_2\}$.

Key words: molecular magnets, spin transitions, copper(II) complexes, hexafluoroacetylacetonates, nitroxide radicals, thermomagnetic measurements, X-ray diffraction.

Solid phases of heterospin complexes based on bis(hexafluoroacetylacetonato)copper(II) $[Cu(hfac)_2]$ with nitronyl nitroxide radicals (NNRs) are of interest because they can undergo structural transformations accompanied by spin transitions induced by external effects.[1,2] Most of known NNRs differ by the substituent R in the 2-imidazoline ring.[3—6] A few heterospin complexes $Cu(hfac)_2$ with NNRs containing Et group(s) in positions of 4 and 5 of the 2-imidazoline ring along with the Me group[7,8] ($L^{Me_2Et_2}$ and L^{Me_3Et}) were documented. In the present study, we describe the synthesis, structures, and magnetic properties of NNRs containing cyclopentane groups in positions 4 and 5 of the imidazoline ring (L^{CP}) and heterospin complexes $Cu(hfac)_2$ with L^{CP}. It should be noted that, along with the above-mentioned modification of hydrocarbon substituents in positions 4 and 5 of the imidazoline ring of L^{CP}, we introduced the pyridin-3-yl substituent in position 2. This allowed us to compare the composition and structure of the solid phases generated in the reactions of $Cu(hfac)_2$ with L^{CP} and L^{Me_4} (or $L^{Me_2Et_2}$, L^{Me_3Et}).

Results and Discussion

With the aim of developing the synthesis of L^{CP}, we followed classical Ullman´s approach[9,10] implying the search for an efficient procedure for the preparation of key 1,2-dihydroxyamine. It should be noted that vicinal dihydroxyamines are scarce. The synthesis of 2,3-bis(hydroxyamino)-2,3-dimethylbutane ($R^{1—4}$ = Me)[11] and racemic mixtures of 2,3-bis(hydroxyamino)-R^2,R^3-butanes ($R^{1—3}$ = Me, R^4 = C_8H_{17}, $MeOCH_2$, $Bu^tPh_2SiOCH_2$, *p*-$MePhCOCH_2$, $PhCOOCH_2$, $MeCOOCH_2$, $HOCH_2$;[12] $R^{2,3}$ = Me, R^1 = Me, Et, R^4 = Et;[7,8] $R^{2,3}$ = Me, R^1 = H, R^4 = Ph)[13] was described earlier. For L^{Me2Et2}, the optical isomers were isolated by separation of intermediate vicinal diamines.[7]

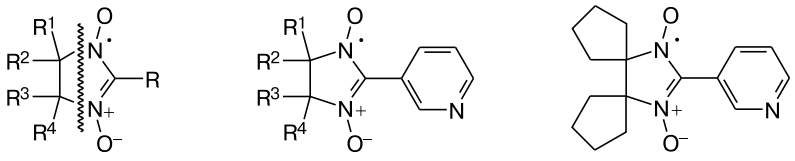

L^{CP}

L^{Me_4}: $R^1 = R^2 = R^3 = R^4$ = Me; $L^{Me_2Et_2}$: $R^1 = R^4$ = Me, $R^2 = R^3$ = Et; L^{Me_3Et}: $R^1 = R^2 = R^3$ = Me, R^4 = Et

Published in Russian in *Izvestiya Akademii Nauk. Seriya Khimicheskaya,* No. 10, pp. 2132—2140, October, 2013.
1066-5285/13/6210-2132

The molecular and crystal structure of 1,1′-dihydroxylamino-bis(cyclopentyl) sulfate monohydrate was determined (Fig. 1). This structure is composed of doubly protonated 1,1′-dihydroxylamino-bis(cyclopentyl) molecules, sulfate anions, and solvate water molecules linked together by a complex system of hydrogen bonds.

Spin-labeled L^{CP} was also isolated as single crystals suitable for X-ray diffraction (Fig. 2). In the L^{CP} molecule, the N—O distances are equal to each other (1.285(2) and 1.283(2) Å), which is typical of NNRs.[14] The angle between the planes of the pyridyl ring and the nitronyl nitroxide moiety $\{O_2N_2C\}$ is 32.7°. The shortest contact between the O atoms of the NO groups of adjacent molecules is 4.044(3) Å. Such long intermolecular distances between the paramagnetic centers in solid L^{CP} are responsible for the almost invariable effective magnetic moment (μ_{eff}), which is equal to 1.74 μ_B in the range of 30—300 K. This value is well consistent with the theoretical spin-only value of 1.73 μ_B for non-interacting paramagnetic centers (PMCs) with the spin $S = 1/2$ and the g-factor of 2.

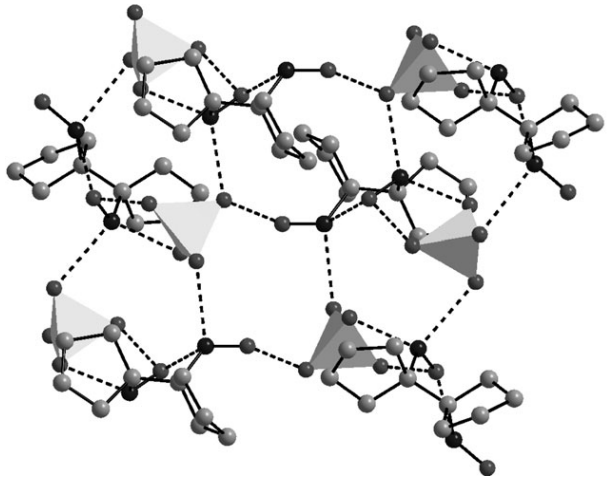

Fig. 1. Fragment of the packing of 1,1′-dihydroxylamino-bis(cyclopentyl) sulfate monohydrate. The dashed lines connect hydrogen-bonded atoms; the H atoms are not shown. The sulfate groups are represented as tetrahedra.

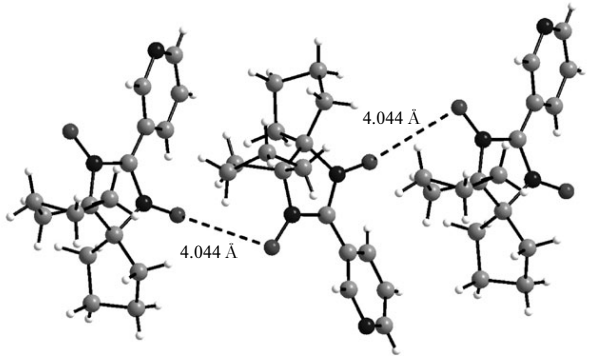

Fig. 2. Fragment of the packing of L^{CP}. The shortest contacts between the O atoms of the NO groups of adjacent molecules are indicated by dashed lines.

In the course of investigation of the $Cu(hfac)_2$—L^{CP} reaction system, we showed that different heterospin complexes can be reproducibly synthesized by varying the ratio of the starting reagents. In most cases, the starting $Cu(hfac)_2 : L^{CP}$ ratio was retained in the final product. This is true for $[Cu(hfac)_2L^{CP}_2]$, $\{[Cu(hfac)_2]_4(L^{CP})_2\}$, and $\{[Cu(hfac)_2]_3(L^{CP})_2\}_n$. Only the synthesis of $[Cu(hfac)_2L^{CP}]_2$, despite the 1 : 1 ratio, resulted in the formation of both $[Cu(hfac)_2L^{CP}]_2$ and $[Cu(hfac)_2L^{CP}_2]$ as solid phases. As mentioned in the Experimental section, the crystals of these complexes were mechanically separated.

The mononuclear complex $[Cu(hfac)_2L^{CP}_2]$ (Fig. 3, *a*) has a structure typical of complexes with this stoichiometry.[8,15,16] In this complex, the N_{Py} atoms of the pyridine rings are in the equatorial plane of the pseudo-centrosymmetric Cu bipyramid. The Cu...N distances are 2.009(5) and 2.012(5) Å. The equatorial Cu—O_{hfac} distances are 2.073(5) and 2.085(5) Å, whereas the axial distances are substantially longer (2.188(5) and 2.189(5) Å, respectively). The intermolecular distances between the paramagnetic centers are rather large. The shortest distances are O(1R)...O(10R′) (4.119(7) Å), O(1S)...O(10S′) (3.817(9) Å), and O(10R)...O(10R″) (3.772(7) Å) (Fig. 3, *b*). The magnetic moment μ_{eff} of $[Cu(hfac)_2L^{CP}_2]$ at room temperature is 3.14 μ_B. It remains virtually unchanged upon lowering the temperature to 50 K and then slightly decreases to 2.75 μ_B at 5 K (Fig. 4). In the range of 300—50 K, the magnetic moment μ_{eff} is close to the theoretical spin-only value for three non-interacting PMCs with $S = 1/2$ and the g-factor of 2. According to the X-ray diffraction data, the experimental dependence $\mu_{eff}(T)$ for $[Cu(hfac)_2L^{CP}_2]$ is best described assuming that exchange interactions occur only between nitroxides (O(10R)...O(10R″); a model of an exchange-coupled dimer for $S = 1/2$), whereas the other PMCs do not interact with each other (the magnetic susceptibility follows the Curie law $\chi = C/T$). The optimal values of the parameters J/k and C are −7.9(±0.3) K and 0.85(±0.01) K cm^3 mol^{-1}, respectively. The Curie constant C agrees well with the theoretical spin-only value of 0.83 K cm^3 mol^{-1} for two non-interacting PMCs, *viz.*, the Cu^{II} ion ($S = 1/2$ with $g = 2.2$) and NNR ($S = 1/2$ with $g = 2$).

The structure of $[Cu(hfac)_2L^{CP}]_2$ is composed of two crystallographically independent centrosymmetric molecules (Fig. 5). At room temperature, the Cu atoms in these molecules are in the same coordination environment. The O atom of the NO group (Cu(1)—O(1R), 2.346(2) Å; and Cu(2)—O(1S) 2.214(2) Å) and one of the O_{hfac} atoms (2.275(3) and 2.251(2) Å) are in the axial positions on the long axis of the Cu bipyramid. The equatorial plane is formed by three O_{hfac} atoms and one N_{Py} atom at distances of 1.952(2)—2.037(2) and 2.017(2)—2.021(2) Å, respectively, from the Cu atom.

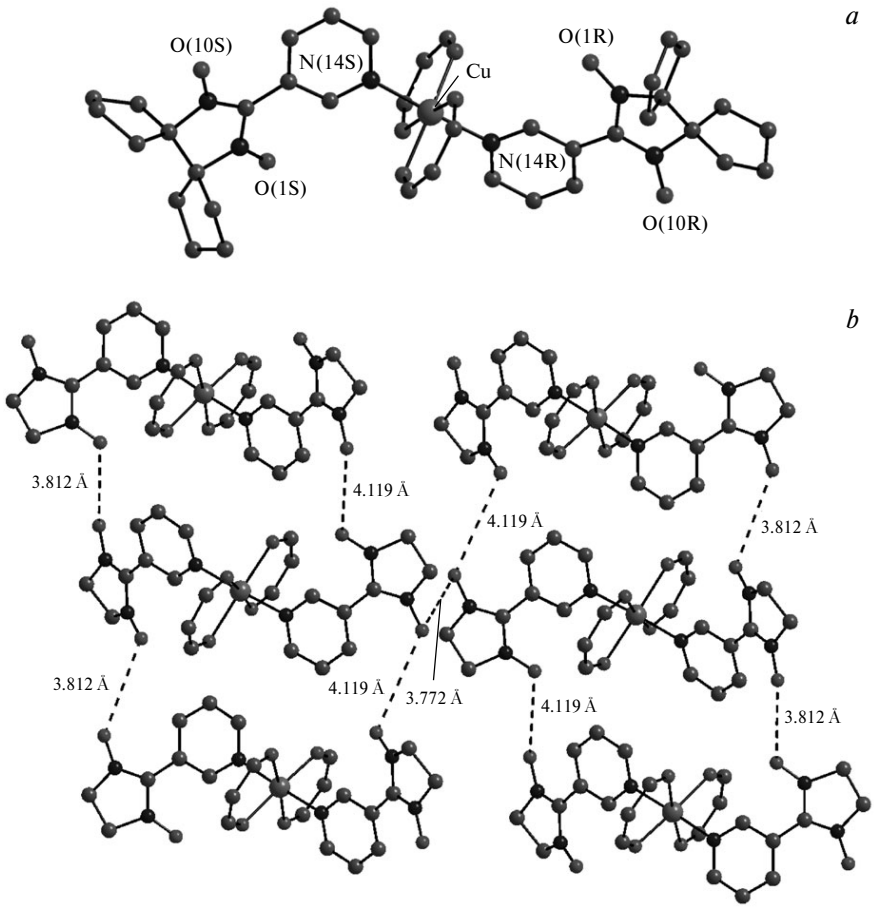

Fig. 3. Molecular structure of $[Cu(hfac)_2L^{CP}{}_2]$ (*a*, the H atoms and the CF_3 groups of hfac are not shown) and the crystal packing (*b*).

The X-ray diffraction study of $[Cu(hfac)_2L^{CP}]_2$ at different temperatures revealed the nontrivial structural dynamics of the coordination units within the binuclear molecules. Upon lowering the temperature from 296 to 75 K, the following changes are observed in the coordination environment of Cu(2): a gradual decrease in the Cu(2)—O(1S) and Cu(2)—O_{hfac} bond lengths from 2.214(2) to 1.970(3) Å and from 2.251(2) to 2.010(3) Å, respectively, accompanied by an elongation of the Cu—O_{hfac} bonds in the perpendicular direction from 2.037(2) to 2.252(3) and from 2.036(2) to 2.280(3) Å. The absolute change in the distances in these directions is larger than 0.2 Å, whereas the changes along the O_{hfac}—Cu(2)—N axis of the octahedron do not exceed 0.016 Å: 1.987(2) → 1.972(3) Å for Cu(2)—O_{hfac} and 2.017(2) → 2.001(4) Å for Cu(2)—N. In the coordination polyhedron of Cu(1), the Jahn-Teller axis switching does not occur, and the observed changes reflect the usual temperature-induced compression of the structure. At 296 K, the shortest O...O distances between the dimers are 3.883(3) Å (see Fig. 5), and they change only slightly with decreasing temperature.

The experimental dependence $\mu_{eff}(T)$ for $[Cu(hfac)_2L^{CP}]_2$ is shown in Fig. 6. At room temperature, μ_{eff} is 3.52 μ_B, which corresponds to four non-interacting PMCs with the spin $S = 1/2$ and $g = 2$. Upon cooling to ~125 K, the value of μ_{eff} gradually decreases to ~2.82 μ_B. This is well consistent with the data on the temperature dynamics of the $[Cu(hfac)_2L^{CP}]_2$ structure. In the range of 300—120 K, the coordinated O_{NO} atoms go from the axial to the equatorial positions in one-half of the crystallographically in-

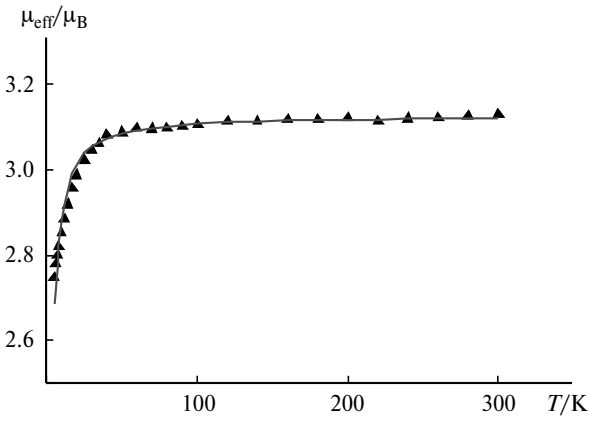

Fig. 4. Experimental dependence $\mu_{eff}(T)$ (points) and the corresponding theoretical curve for $[Cu(hfac)_2L^{CP}{}_2]$.

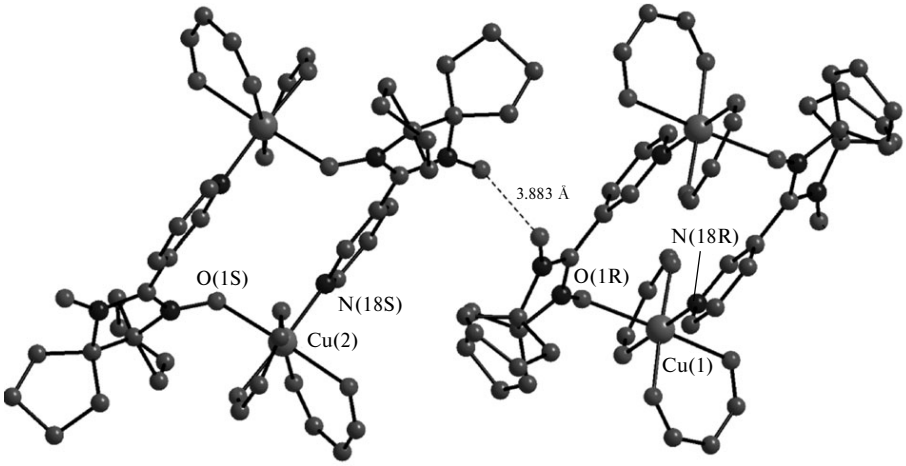

Fig. 5. Molecular structure of $[Cu(hfac)_2L^{CP}]_2$ (the H atoms and the CF_3 groups of hfac are not shown).

dependent dimers $[Cu(hfac)_2L^{CP}]_2$, giving rise to strong antiferromagnetic exchange in the >N—·O—Cu^{2+} exchange clusters and, as a consequence, resulting in the complete spin compensation in this half of the molecules. The geometry of the coordination units in the molecules $[Cu(hfac)_2L^{CP}]_2$ of the second type is favorable for the ferromagnetic exchange due to which the μ_{eff} value at ~125 K is close to the theoretical value of 2.83 μ_B for a paramagnetic material containing PMCs with $S = 1$ ($g = 2$). As the temperature is further lowered, μ_{eff} increases. This fact confirms the presence of intramolecular ferromagnetic exchange in the second half of the dimeric molecules, in which no spin pairing of copper(II) and coordinated nitroxyl occurs.

It should be noted that spin transitions were observed earlier[7,17,18] in heterospin dimers containing >N—·O—Cu^{2+} exchange clusters. From this point of view, the results of the present study extend the range of such compounds. However, the behavior of the curve $\mu_{eff}(T)$ for $[Cu(hfac)_2L^{CP}]_2$ (see Fig. 6) is not typical of spin transitions, and this pattern was observed for the first time for a heterospin solid phase formed by dimers from >N—·O—Cu^{2+} exchange clusters. In addition, the phase transition found in $[Cu(hfac)_2L^{CP}]_2$ is reversible, as opposed to those described earlier[7] for cyclic dimers containing similar NNRs, *viz.*, L^{Me_3Et} and $L^{Me_2Et_2}$. Single crystals of the complex $[Cu(hfac)_2L^{CP}]_2$, despite a small hysteresis (inset in Fig. 6) accompanying the phase transformation, have high mechanical stability. This is yet another useful characteristic of this compound, which allowed us to study the relationship between the structural dynamics and the changes in the magnetic properties using one and the same crystal.

Therefore, the results of our study showed that the temperature-induced structural rearrangement provoking the spin transition occurs in one-half of the dimeric molecules in solid $[Cu(hfac)_2L^{CP}]_2$. The fact that the observed magnetic effect is a consequence of a substantial structural reorganization of only one-half of the $[Cu(hfac)_2L^{CP}]_2$ molecules is another previously unknown distinguishing features of heterospin complexes.[1]

The solid phase $[Cu(hfac)_2]_4(L^{CP})_2]$ is formed by tetranuclear molecules (Fig. 7). They are structurally similar to the $[Cu(hfac)_2L^{CP}]_2$ molecules (see Fig. 5) with the only difference that all four O atoms of two bridging ligands L^{CP} are coordinated to Cu atoms of four different $Cu(hfac)_2$ fragments. Complexes having the same composition and structure were synthesized earlier[7,17,18] with NNRs L^{Me_4}, $L^{Me_2Et_2}$, and L^{Me_3Et}. Spin transitions were found in all these complexes. It should be emphasized that it is $\{[(Cu(hfac)_2]_2L^{Me4}\}_2$, where the dependence $\mu_{eff}(T)$ typical of spin transitions in classical systems[17] was observed for the first time.

The coordination environment of the terminal Cu atoms in the $\{[Cu(hfac)_2]_4(L^{CP})_2\}$ molecules can be described as a square pyramid with the O_{NO} atom in the apical position (Cu(1)—O(1R), 2.332(2) Å) and four O_{hfac} atoms in the equatorial plane (Cu—O_{hfac}, 1.915(2)—1.938(2) Å). The

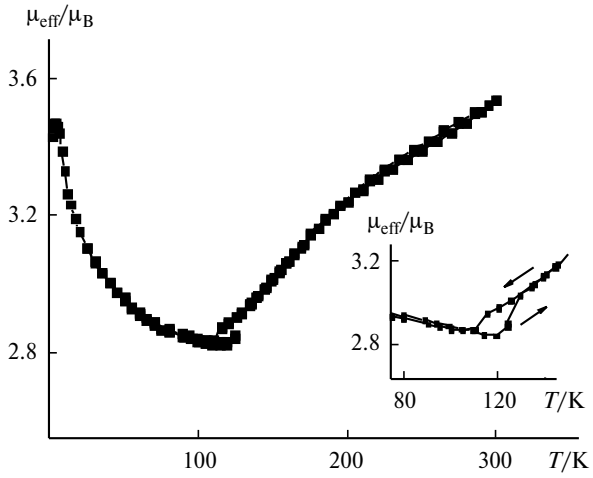

Fig. 6. Experimental dependence $\mu_{eff}(T)$ for $[Cu(hfac)_2L^{CP}]_2$. The inset shows the hysteresis in the transition region.

long axis of the square bipyramid of the Cu(2) atom involved in the 14-membered metallocycle (see Fig. 7) is formed, like in $[Cu(hfac)_2L^{CP}]_2$, by the O_{NO} and O_{hfac} atoms (Cu(2)—O(2R), 2.403(2) Å; Cu(2)—O_{hfac}, 2.284(2) Å). Upon cooling of the crystal from 296 to 110 K, the axial bond lengths decrease: Cu(1)—O(1R) from 2.332(2) to 2.296(1) Å, Cu(2)—O_{hfac} from 2.284(2) to 2.262(1) Å, and Cu(2)—O(2R) from 2.403(2) to 2.311(1) Å. A further decrease in the temperature to 75 K leads to an abrupt shortening of the Cu(2)—O(2R) and Cu(2)—O_{hfac} bonds by 0.3 and 0.25 Å, respectively. Simultaneously, the Cu(1)—O(1R) bond is elongated by more than 0.07 Å. Despite substantial rearrangements of the coordination units and the sharpness of the phase transition at 100 K (Fig. 8), the crystals remain unchanged upon the repeated cooling—heating cycle, which enabled us to follow their structural dynamics.

The dependence $\mu_{eff}(T)$ for $\{[Cu(hfac)_2]_4(L^{CP})_2\}$ is shown in Fig. 8. In the temperature range of 100—300 K, μ_{eff} remains virtually unchanged and is 4.0 μ_B, which is close to the theoretical spin-only value of 4.24 μ_B for six non-interacting PMCs with the spin $S = 1/2$ and $g = 2$. At temperatures below 100 K, μ_{eff} sharply decreases and reaches a plateau of 2.54 μ_B in the temperature range 80—5 K. The value $\mu_{eff} = 2.54\ \mu_B$ corresponds to two independent spins $S = 1/2$. This is fully consistent with the data on the structural rearrangement of $\{[Cu(hfac)_2]_4(L^{CP})_2\}$, during which the coordinated O_{NO} atoms go from the axial to the equatorial positions and which is known[13,19] to be responsible for the appearance of strong antiferromagnetic exchange interactions in the >N—·O—Cu^{2+} exchange clusters, resulting, in turn, in the complete spin compensation of PMCs in the {Cu(2)—O(2R)} moieties.

The spin transitions inherent in the complexes $[Cu(hfac)_2L^{CP}]_2$ and $\{[Cu(hfac)_2]_4(L^{CP})_2\}$ are accompanied by thermochromic effects. The spontaneous heating of a powdered sample of $[Cu(hfac)_2L^{CP}]_2$ deposited on a paper and cooled to the liquid nitrogen temperature leads to a change in the tint of the color of the sample from brown to greenish-brown. For $\{[Cu(hfac)_2]_4(L^{CP})_2\}$, the change in the color of the sample subjected to the similar treatment is more pronounced. Thus, the color sharply changes from dark-red to green.

In addition to the above-described compounds, we isolated the heterospin complex $\{[Cu(hfac)_2]_3(L^{CP})_2\}_n$ with the $[Cu(hfac)_2] : L^{CP}$ ratio of 3 : 2. The solid phase also contains the cyclic dimers $[(Cu(hfac)_2L^{CP}]_2$, which are linked by $Cu(hfac)_2$ groups coordinating the free O_{NO} atoms to form chains (Fig. 9). The coordination environment of the Cu(1) atom is similar to that in $[(Cu(hfac)_2L^{CP}]_2$, *i.e.*, two O_{hfac} atoms form the long axis of the bipyramid (Cu(1)—O_{hfac}, 2.254(2) and 2.350(2) Å), and the distances to the atoms of the paramagnetic ligands, Cu(1)—O(1R) and Cu(1)—N(18R), are short (1.999(2) and 1.986(2) Å, respectively). The apical positions of the centrosymmetric bipyramid of Cu(2) are occupied by the O_{NO} atoms with the Cu(2)—O(14R) distance of 2.586(2) Å. The X-ray diffraction studies of the complex at 323, 295, 240, 175, and 130 K revealed no significant changes in the structural parameters.

The value of μ_{eff} for $\{[Cu(hfac)_2]_3(L^{CP})_2\}_n$ at 350 K is 2.42 μ_B, it gradually decreases with decreasing temperature and reaches 1.98 μ_B at 5 K (Fig. 10). The high-temperature value of μ_{eff} is substantially smaller than the theoretical spin-only value of 3.87 μ_B for five non-interacting PMCs with the spins $S = 1/2$ and the g-factor of 2. This behavior of $\mu_{eff}(T)$ is indicative of the presence of strong antiferromagnetic exchange interactions, which is consistent with the X-ray diffraction data (the short Cu(1)—O(1R) distance). Hence, the spins in the solid phase $\{[Cu(hfac)_2]_3(L^{CP})_2\}_n$ are partially compensated already at room temperature, and the paramagnetism of the compound is determinedly only by the spins of the exocyclic Cu^{2+} ions.

In conclusion, we synthesized the nitroxide radical L^{CP} bearing cyclopentane groups in positions 4 and 5 of the

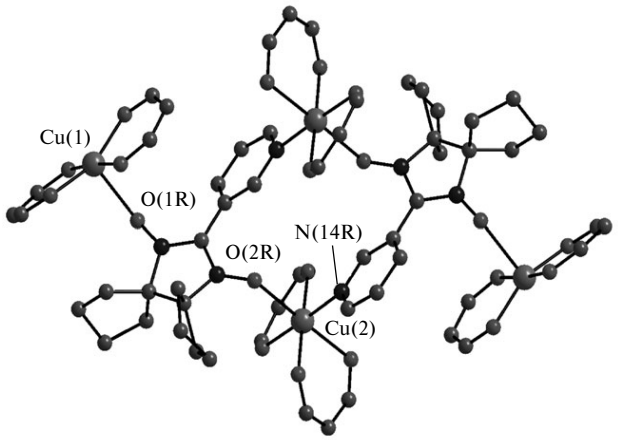

Fig. 7. Molecular structure of $\{[Cu(hfac)_2]_4(L^{CP})_2\}$ (the H atoms and the CF_3 groups of hfac are not shown).

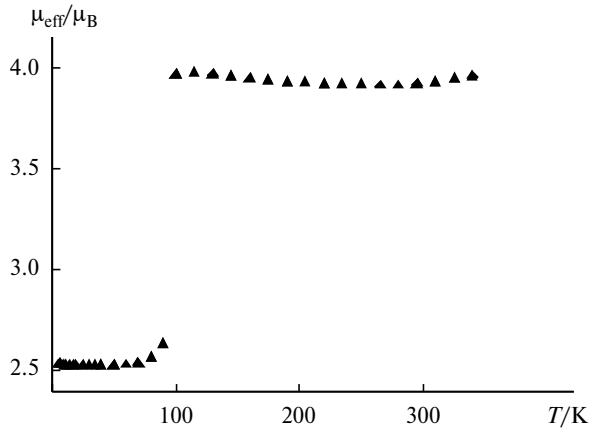

Fig. 8. Experimental dependence $\mu_{eff}(T)$ for the complex $\{[Cu(hfac)_2]_4(L^{CP})_2\}$.

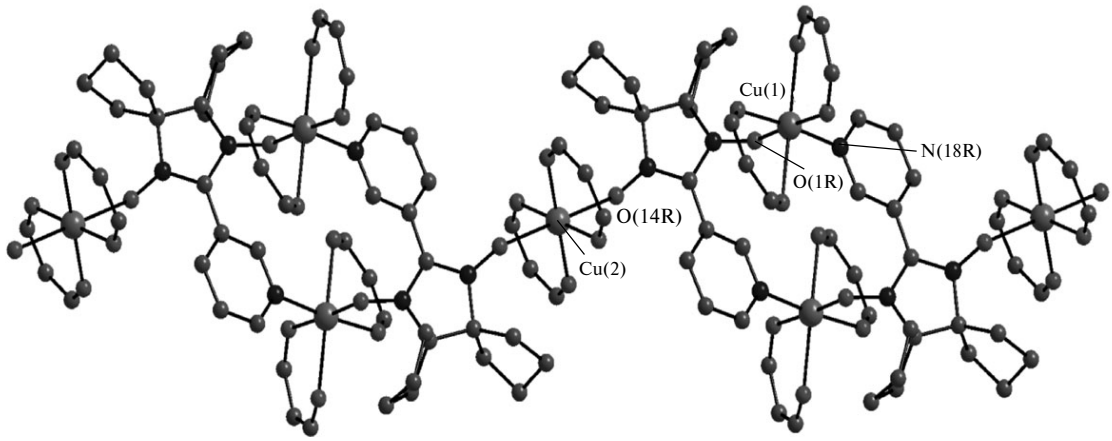

Fig. 9. Fragment of the chain $\{[Cu(hfac)_2]_3(L^{CP})_2\}_\infty$ (the H atoms and the CF_3 groups of hfac are not shown).

imidazoline ring and isolated heterospin compounds based on $Cu(hfac)_2$ with L^{CP}, which can undergo thermally induced spin transitions. It was shown that high mechanical stability of the solid samples of $[Cu(hfac)_2L^{CP}]_2$ and $\{[(Cu(hfac)_2]_4(L^{CP})_2\}$ allows single crystal-to-single crystal phase transitions to occur upon repeated cooling—heating cycles.[20—23]

Experimental

Nitrocyclopentane[24] and bis(hexafluoroacetylacetonato)-copper(II)[25] were synthesized according to known procedures; commercial reagents and solvents were used as is without further purification.

Chromatography was performed using silica gel 60 F_{254}, aluminum sheets for TLC (Macherey-Nagel), silica gel (0.063—0.200 mm) for column chromatography, Merck), and Al_2O_3 (chromatography grade, Donetsk Plant of Chemical Reagents, Ukraine). The IR spectra were recorded on a Bruker Vector-22 spectrophotometer as KBr pellets. The melting points were measured on a Stuart hot-stage microscope apparatus. The microanalyses were carried out on a EURO EA3000 CHNS-analyzer at the N. N. Vorozhtsov Novosibirsk Institute of Organic Chemistry of the Siberian Branch of the Russian Academy of Sciences. The NMR spectra were recorded on a Bruker AV-400 instrument.

The magnetic susceptibility of polycrystalline samples was measured on a Quantum Design MPMS*XL* SQUID magnetometer in the temperature range of 2—300 K at a magnetic field strength of 5 kOe. The paramagnetic components of the magnetic susceptibility χ were determined taking into account the diamagnetic contribution estimated using the Pascal additive scheme. The temperature-dependent effective magnetic moment was calculated according to the equation

$$\mu_{eff}(T) = [(3k/N\mu_B^2)\chi T]^{0.5} \approx (8\chi T)^{0.5},$$

where N_A is Avogadro´s number, k is the Boltzmann constant, and μ_B is the Bohr magneton.

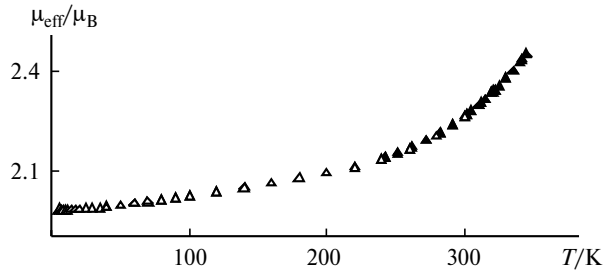

Fig. 10. Experimental dependence $\mu_{eff}(T)$ for $\{[Cu(hfac)_2]_3(L^{CP})_2\}_\infty$.

The compound L^{CP} was synthesized according to Scheme 1.

1,1´-Dinitrobicyclopentane. Nitrocyclopentane (5.71 g, 0.05 mol) was added to a suspension of Bu^tOK (5.60 g, 0.05 mol) in DMF (30 mL) with cooling. Then a solution of I_2 (6.35 g, 0.025 mol) in DMF (20 mL) was added dropwise with stirring. The reaction mixture was kept at ~20 °C for 2 h, and then water (~150 mL) was added. The product was filtered off, washed with water, and dissolved in Et_2O. The solution was washed with a 10% aqueous $Na_2S_2O_3$ solution (2×30 mL). The organic layer was separated and dried over anhydrous Na_2SO_4. The solution was passed through a silica gel layer (1.5×10 cm), and the eluate was concentrated *in vacuo*. The residue was crystallized from a Et_2O—hexane mixture. The yield was 2.8 g (50%), colorless needles, m.p. 80—82 °C (decomp.). Found (%): C, 52.7; H, 7.0; N, 12.2. $C_{10}H_{16}N_2O_4$. Calculated (%): C, 52.6; H, 7.1; N, 12.3. IR, ν/cm^{-1}: 2950, 2875, 1555, 1471, 1451, 1435, 1361, 1333, 1313, 1191, 1060, 954, 936, 911, 852, 751, 665, 552, 426. ^1H NMR (100 MHz, $CDCl_3$), δ: 2.8—2.6 (m, 4 H); 2.2—1.6 (m, 12 H).

1,1´-Dihydroxylamino-bis(cyclopentyl) sulfate monohydrate. The compounds NH_4Cl (1.92 g, 0.036 mol) and $CdSO_4$ (0.020 g, 0.0096 mmol) were added to a solution of 1,1´-dinitrobicyclopentane (2.00 g, 8.8 mmol) in THF (60 mL) and water (6.0 mL). The mixture was cooled to 15 °C, and then a zinc powder (3.12 g, 0.048 mol) was added portionwise with stirring for 30 min. The reaction mixture was stirred for 1 h and filtered. The precipitate was washed with THF (3×20 mL). The filtrate was concentrated *in vacuo*, and the residue was dissolved in acetone (30 mL) and filtered. A 20% H_2SO_4 solution in EtOH was added dropwise with stirring to the reaction solution until the pH was adjusted to 3 (Thymol Blue). Small colorless needle-like crystals that formed were filtered off, washed with acetone, and dried in air. The yield was 1.13 g (41%). The product was recrystallized

Scheme 1

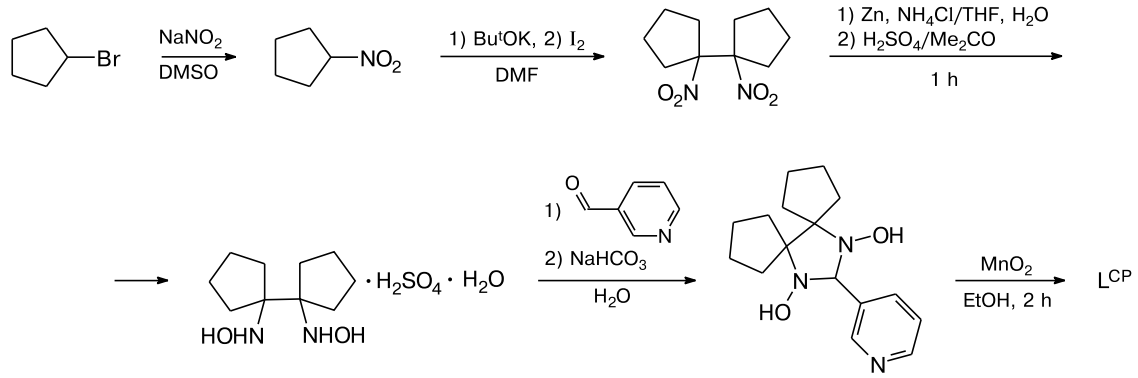

from a EtOH—H_2O solvent mixture. The yield was 0.4 g, m.p. 178—180 °C (decomp.). Found (%): C, 37.9; H, 7.6; N, 8.8. $C_{10}H_{24}N_2O_7S$. Calculated (%): C, 38.0; H, 7.7; N, 8.9. IR, ν/cm^{-1}: 3486, 2977, 2886, 2723, 1616, 1563, 1503, 1477, 1433, 1337, 1126, 1090, 1047, 1005, 981, 970, 943, 913, 778, 604, 534, 452, 419.

2-(3-Pyridyl)-4,5-bis(spiropentyl)-4,5-dihydro-1*H*-imidazole-3-oxide-1-oxyl (L^{CP}). 1,1′-Dihydroxylamino-bis(cyclopentyl) sulfate monohydrate (150 mg, 0.5 mmol) was dissolved in water (3 mL), and pyridine-3-carbaldehyde (55.0 mg, 0.5 mmol) was added. The reaction mixture was stirred at ~20 °C for 1 h and then neutralized with $NaHCO_3$ until the gas evolution ceased. The precipitate that formed was filtered off, washed with water, and dried in air and then in a vacuum chamber. 2-(3-Pyridyl)-4,5-bis(spiropentyl)-4,5-dihydro-1*H*-imidazolidine-1,3-diol was obtained as a white powder in a yield of 55 mg. An excess of MnO_2 (270 mg) was added to a suspension of this product in MeOH (3 mL). The suspension was stirred for 1 h with cooling in a water bath. The resulting solution was filtered from an excess of MnO_2. The residue was washed on the filter with MeOH, and the filtrate was concentrated to dryness. The dry residue was dissolved in EtOAc and filtered through a silica gel layer (2×5 cm). The eluate was concentrated using a rotary evaporator. The product was crystallized from a Et_2O—hexane mixture at 4 °C. The yield was 38 mg (28%), prismatic dark-blue crystals. M.p. 82—85 °C (decomp.). Found (%): C, 67.0; H, 7.0; N, 14.7. $C_{16}H_{20}N_3O_2$. Calculated (%):C, 67.1; H, 7.0; N, 14.7. IR, ν/cm^{-1}: 3448, 2964, 2948, 2871, 1590, 1565, 1462, 1440, 1422, 1409, 1384, 1349, 1333, 1314, 1177, 1141, 1118, 1027, 952, 920, 862, 823, 806, 759, 702, 636, 610, 566, 540.

Synthesis of complexes. Complex [Cu(hfac)$_2$(L^{CP})$_2$]. Hexane (5 mL) was added to a solution of $Cu(hfac)_2$ (15 mg, 0.031 mmol) and L^{CP} (21 mg, 0.063 mmol) in CH_2Cl_2 (1 mL). The resulting solution was kept in an open vessel at 4 °C for one day. Needle-like green crystals that formed were filtered off, washed with cold hexane, and dried in air. The yield was 30.5 mg (85%). M.p. 160—162 °C (decomp.). Found (%): C, 48.0; H, 4.0; F, 21.8; N, 7.9. $C_{42}H_{42}CuF_{12}N_6O_8$. Calculated (%): C, 48.0; H, 4.0; F, 21.7; N, 8.0.

Complex [Cu(hfac)$_2$$L^{CP}$]$_2$. $Cu(hfac)_2$ (30 mg, 0.063 mmol) was dissolved in hexane (3.0 mL) upon heating to 50 °C, and then a solution of L^{CP} (21 mg, 0.063 mmol) in CH_2Cl_2 (1.0 mL) was added. The reaction mixture was kept in an open vessel at 4 °C for one day, after which platelet-like dark-red crystals of the target complex $[Cu(hfac)_2L^{CP}]_2$ and crystals of the above-described $[Cu(hfac)_2(L^{CP})_2]$ formed. The crystals were filtered off, washed with cold hexane, dried in air, and mechanically separated. The yield was 20 mg (40 %). M.p. 118—120 °C (decomp.). Found (%): C, 41.0; H, 2.9; F, 29.4; N, 5.5. $C_{52}H_{44}Cu_2F_{24}N_6O_{12}$. Calculated(%): C, 40.9; H, 2.9; F, 29.8; N, 5.5.

Complex {[Cu(hfac)$_2$]$_3$(L^{CP})$_2$}$_n$ was synthesized by the reaction of $Cu(hfac)_2$ (45 mg, 0.095 mmol) with L^{CP} (21 mg, 0.063 mmol). The yield was 40 mg (60 %), dark-red prismatic crystals. M.p. 116—118 °C (decomp.). Found (%): C, 37.2; H, 2.2; F, 34.0; N, 4.2. $C_{62}H_{46}Cu_3F_{36}N_6O_{16}$. Calculated (%): C, 37.1; H, 2.3; F, 34.1; N, 4.2.

Complex {[Cu(hfac)$_2$]$_4$(L^{CP})$_2$} was synthesized by the reaction of $Cu(hfac)_2$ (41 mg, 0.085 mmol) with L^{CP} (14 mg, 0.042 mmol) by analogy with the synthesis of $[Cu(hfac)_2(L^{CP})_2]$. The yield was 36 mg (65%), dark-green crystals. M.p. 126—128 °C (decomp.). Found (%): C, 34.5; H, 2.1; F, 36.6; N, 3.2. $C_{72}H_{48}Cu_4F_{48}N_6O_{20}$. Calculated (%): C, 34.8; H, 2.0; F, 36.7; N, 3.4.

X-ray diffraction study. Single-crystal X-ray diffraction data sets were collected on a Bruker AXS SMART APEX II diffractometer equipped with an Oxford Cryosystems Helix low-temperature device and on an APEX DUO diffractometer; absorption corrections were applied using the SADABS program, version 2.10. The structures were solved by direct methods and refined by the full-matrix least-squares method with anisotropic displacement parameters for all nonhydrogen atoms. In most of the structures, the hydrogen atoms were positioned geometrically and refined using a riding model. In all structures, the rotational disorder of CF_3 groups of the hexafluoroacetylacetonate ligands was observed in the temperature range of 300—120 K. All calculations associated with the structure solution and refinement were carried out using the Bruker Shelxtl Version 6.14 program package. Crystallographic characteristics and the X-ray data collection and structure refinement statistics are given in Tables 1—3.

This study was financially supported by the Russian Foundation for Basic Research (Project Nos 12-03-00067, 11-03-00027, and 12-03-31028), the Ministry of Education and Science of the Russian Federation (Agreement 8436), the Council on Grants at the President of the Russian Federation (Program for State Support of Young Scientists, Grants MK-6497.2012.3 and MK-1165.2012.3), the Russian Academy of Sciences, and the Siberian Branch of the Russian Academy of Sciences.

Table 1. Crystallographic characteristics and the X-ray data collection and structure refinement statistics for $[Cu(hfac)_2L^{Cp}]_2$ at different temperatures/K

Parameter	295	240	175	120	75
Molecular weight	1528.02	1528.02	1528.02	1528.02	1528.02
Space group	*P*-1	*P*-1	*P*-1	*P*-1	*P*-1
Z	2	2	2	2	2
a/Å	13.4200(9)	13.4066(5)	13.399(1)	13.8628(9)	13.878(1)
b/Å	15.3457(10)	15.2309(6)	15.094(1)	14.8358(10)	14.734(1)
c/Å	17.1578(11)	17.0921(7)	16.985(1)	16.2797(11)	16.258(1)
α/deg	72.492(4)	72.382(3)	72.350(2)	72.998(4)	73.121(7)
β/deg	70.770(4)	70.474(3)	70.014(2)	71.413(4)	71.301(6)
γ/deg	81.845(4)	81.242(3)	80.673(2)	79.905(4)	79.787(7)
V/Å	3178.2(4)	3130.0(2)	3069.5(4)	3022.4(3)	3000.3(5)
d_{calc}/g cm^{-3}	1.597	1.621	1.653	1.679	1.691
μ/mm^{-1}	2.031 (Cu)	0.813	0.829	0.842	0.849
θ_{max}/deg	64.00	28.53	28.17	27.50	28.22
I_{hkl} (measured/unique)	37844/10242	70964/15634	53319/14888	46060/13656	37342/13579
R_{int}	0.0767	0.1186	0.0832	0.0914	0.1487
I_{hkl} ($I > 2\sigma_I$)	6748	4760	6424	7038	5542
N	1081	1090	1054	964	865
GOOF	1.025	0.628	0.757	0.899	0.855
R_1	0.0483	0.0376	0.0417	0.0532	0.0568
wR_2 ($I > 2\sigma$)	0.1277	0.0695	0.0708	0.1142	0.0996
R_1	0.0720	0.1854	0.1217	0.1149	0.1631
wR_2	0.1390	0.1043	0.0854	0.1346	0.1283

Table 2. Crystallographic characteristics and the X-ray data collection and structure refinement statistics for $[Cu(hfac)_2L^{CP}_2]$ at 296 K and for $\{[Cu(hfac)_2]_4(L^{CP})_2\}$ at different temperatures/K

Parameter	$[Cu(hfac)_2L^{CP}_2]$	$\{[Cu(hfac)_2]_4(L^{CP})_2\}$			
		295	240	110	75
Molecular weight	1050.36	1241.66	1241.66	1241.66	1241.66
Space group	*Pbca*	*P*-1	*P*-1	*P*-1	*P*-1
Z	8	2	2	2	2
T/K	296	295	240	110	75
a/Å	12.1224(5)	11.6579(10)	11.5939(5)	11.5287(10)	11.5467(9)
b/Å	14.7836(7)	13.1091(13)	13.0336(5)	12.8624(11)	12.5792(10)
c/Å	51.792(2)	16.2114(15)	16.1654(7)	16.1271(14)	16.1967(13)
α/deg	90	71.411(6)	71.027(2)	70.271(4)	69.858(5)
β/deg	90	81.163(6)	80.861(2)	80.369(4)	79.610(5)
γ/deg	90	84.776(7)	84.512(2)	83.947(4)	82.756(5)
V/Å	9281.9(7)	2318.0(4)	2278.19(16)	2216.2(3)	2167.2(3)
d_{calc}/g cm^{-3}	1.503	1.779	1.810	1.861	1.903
μ/mm^{-1}	1.613 (Cu)	1.071	1.089	1.120	1.145
θ_{max}/deg	4.03—54.00	28.37	28.02	28.19	28.44
I_{hkl} (measured/unique)	26682/5423	26809/11073	38458/10813	37673/10699	34710/10735
R_{int}	0.1240	0.0607	0.0466	0.0442	0.0630
I_{hkl} ($I > 2\sigma_I$)	2886	5279	6191	9039	6826
N	704	811	811	793	676
GOOF	0.951	0.826	0.859	1.032	0.893
R_1	0.0698	0.0391	0.0375	0.0290	0.0384
wR_2 ($I > 2\sigma_I$)	0.1775	0.0678	0.0696	0.0804	0.0651
R_1	0.1259	0.1025	0.0760	0.0358	0.0734
wR_2	0.1991	0.0788	0.0769	0.0832	0.0716

Table 3. Crystallographic characteristics and the X-ray data collection and structure refinement statistics for $\{[Cu(hfac)_2]_3(L^{CP})_2\}_n$ at different temperatures/K and for L^{CP} at 296 K

Parameter	$\{[Cu(hfac)_2]_3(L^{CP})_2\}_n$					L^{CP}
	323	295	240	175	130	
Molecular weight	2005.66	2005.66	2005.66	2005.66	2005.66	286.35
Space group	$P2_1/c$	$P2_1/c$	$P2_1/c$	$P2_1/c$	$P2_1/c$	$P2_1/c$
Z	2	2	2	2	2	4
a/Å	15.592(4)	15.5623(4)	15.4920(6)	15.4049(4)	15.3512(6)	10.320(3)
b/Å	12.750(4)	12.6740(3)	12.5807(5)	12.4738(4)	12.4106(4)	11.989(3)
c/Å	20.830(7)	20.7792(6)	20.7413(8)	20.6940(5)	20.6803(8)	12.277(3)
β/deg	107.586(9)	107.251(2)	107.124(3)	107.032(2)	107.039(2)	104.77(2)
V/Å	3947(2)	3914.0(2)	3863.3(3)	3802.1(2)	3767.0(2)	1468.8(7)
d_{calc}/g cm^{-3}	1.687	1.702	1.724	1.752	1.738	1.295
μ/mm^{-1}	0.951	2.343 (Cu)	0.972	0.988	0.997	0.087
θ_{max}/deg	2.05—26.46	2.97—59.00	1.92—28.29	1.38—28.23	1.94—28.40	28.13
I_{hkl} (measured/unique)	27476/8074	31059/5512	36029/9462	36295/9354	34875/9373	12670/3533
R_{int}	0.0403	0.1450	0.1170	0.0944	0.0951	0.1160
I_{hkl} ($I > 2\sigma_I$)	5634	4620	3246	3849	3660	1022
N	718	719	665	611	584	191
GOOF	1.014	1.016	0.712	0.603	0.724	0.738
R_1	0.0392	0.0527	0.0469	0.0453	0.0456	0.0428
wR_2 ($I > 2\sigma_I$)	0.0913	0.1435	0.0644	0.1043	0.0643	0.0808
R_1	0.0671	0.0592	0.1637	0.1307	0.1557	0.2204
wR_2	0.1030	0.1491	0.0807	0.1498	0.0800	0.1112

References

1. V. I. Ovcharenko, E. G. Bagryanskaya, in *Spin-Crossover Materials: Properties and Applications,* Ed. M. Halcrow, John Wiley and Sons Ltd, Chichester, UK, 2013.
2. M. V. Fedin, S. L. Veber, R. Z. Sagdeev, V. I. Ovcharenko, E. G. Bagryanskaya, *Russ. Chem. Bull.* (*Int. Ed.*), 2010, **59**, 1065 [*Izv. Akad. Nauk, Ser. Khim.*, 2010, 1043].
3. P. Rey, V. I. Ovcharenko, in *Magnetism: Molecules to Materials*, *IV*, Eds J. S. Miller, M. Drillon, Wiley-VCH, New York, 2003.
4. V. I. Ovcharenko, K. Yu. Maryunina, S. V. Fokin, E. V. Tretyakov, G. V. Romanenko, V. N. Ikorskii, *Russ. Chem. Bull.* (*Int. Ed.*), 2004, **53**, 2406 [*Izv. Akad. Nauk*, *Ser. Khim.*, 2004, 2304].
5. E. V. Tretyakov, V. I. Ovcharenko, *Russ. Chem. Rev.,* 2009, **78**, 971.
6. V. I. Ovcharenko, in *Stable Radicals: Fundamentals and Applied Aspects of Odd-Electron Compounds*, Ed. R. Hicks, John Wiley and Sons Ltd., Chichester, UK, 2010.
7. C. Hirel, L. Li, P. Brough, K. Vostrikova, J. Pécaut, B. Mehdaoui, M. Bernard, P. Turek, P. Rey, *Inorg. Chem.*, 2007, **46**, 7545.
8. C. Hirel, J. Pécaut, S. Choua, P. Turek, D. B. Amabilino, J. Veciana, P. Rey, *Eur. J. Org. Chem.*, 2005, **2**, 348.
9. E. F. Ullman, J. H. Osiecki, D. G. B. Boocock, R. J. Darcy, *J. Am. Chem. Soc.*, 1972, **20**, 7049.
10. US Pat. 3927019; *Chem. Abstrs*, 1976, **84**, 180213.
11. V. I. Ovcharenko, S. V. Fokin, G. V. Romanenko, I. V. Korobkov, P. Re, *Russ. Chem. Bull.* (*Int. Ed.*), 1999, **48**, 1519 [*Izv. Akad. Nauk, Ser. Khim.*, 1999, 1539].
12. H. Matsuura, R. Tamura, J. Yamauchi, *Synth. Metals*, 2003, **133**, 605.
13. C. Lescop, D. Luneau, V. Ovcharenko, G. Romanenko, Y. Shvedenkov, P. Rey, *C. R. Acad. Sci. Paris, Chemie/Chem.*, 2001, **4**, 215.
14. *Cambridge Structural Database, Version 5.34*, Cambridge Crystallographic Data Center, Cambridge, November 2012 (last update February 2013).
15. D. A. Souza, Y. Moreno, E. A. Ponzio, J. A. L. C. Resende, A. K. Jordã, A. C. Cunha, V. F. Ferreira, M. A. Novak, M. G. F. Vaz, *Inorg. Chim. Acta*, 2011, **370***,* 469.
16. I. Yeltsov, V. Ovcharenko, V. Ikorskii, G. Romanenko, S. Vasilevsky, *Polyhedron*, 2001, **20**, 1215.
17. F. Lanfranc de Panthou, E. Belorizky, R. Calemczuk, D. Luneau, C. Marcenat, E. Ressouche, P. Turek, P. Rey, *J. Am. Chem. Soc.*, 1995, **117**, 11247.
18. F. Lanfranc de Panthou, D. Luneau, R. Musin, L. Öhrström, A. Grand, P. Turek, P. Rey, *Inorg. Chem.*, 1996, **35**, 3484.
19. V. I. Ovcharenko, G. V. Romanenko, K. Yu. Maryunina, A. S. Bogomyakov, E. V. Gorelik, *Inorg. Chem.*, 2008, **47**, 9537.
20. V. I. Ovcharenko, S. V. Fokin, E. T. Kostina, G. V. Romanenko, A. S. Bogomyakov, E. V. Tretyakov, *Inorg. Chem.*, 2012, **51**, 12188.
21. J. W. Lauher, F. W. Fowler, N. S. Goroff, *Acc. Chem. Res.*, 2008, **41**, 1215.
22. K. Tanaka, F. Toda, *Chem. Rev.*, 2000, **100**, 1025.
23. *Reactivity of Molecular Solids,* Eds E. V. Boldyreva, V. V. Boldyrev, Wiley, Chichester, UK, 1999.
24. N. Kornblum, J. W. Powers, *J. Org. Chem.*, 1957, **22**, 455.
25. J. A. Bertrand, R. I. Kaplan, *Inorg. Chem.*, 1966, **5**, 489.

Received April 12, 2013;
in revised form July 3, 2013